

# On the Anatomy of MCMC-Based Maximum Likelihood Learning of Energy-Based Models

Erik Nijkamp\*, Mitch Hill\*, Tian Han, Song-Chun Zhu, and Ying Nian Wu

UCLA Department of Statistics  
8117 Math Sciences Bldg.  
Los Angeles, CA 90095-1554  
(\*equal contributions)

## Abstract

This study investigates the effects of Markov chain Monte Carlo (MCMC) sampling in unsupervised Maximum Likelihood (ML) learning. Our attention is restricted to the family of unnormalized probability densities for which the negative log density (or energy function) is a ConvNet. We find that many of the techniques used to stabilize training in previous studies are not necessary. ML learning with a ConvNet potential requires only a few hyper-parameters and no regularization. Using this minimal framework, we identify a variety of ML learning outcomes that depend solely on the implementation of MCMC sampling.

On one hand, we show that it is easy to train an energy-based model which can sample realistic images with short-run Langevin. ML can be effective and stable even when MCMC samples have much higher energy than true steady-state samples throughout training. Based on this insight, we introduce an ML method with purely noise-initialized MCMC, high-quality short-run synthesis, and the same budget as ML with informative MCMC initialization such as CD or PCD. Unlike previous models, our energy model can obtain realistic high-diversity samples from a noise signal after training.

On the other hand, ConvNet potentials learned with non-convergent MCMC do not have a valid steady-state and cannot be considered approximate unnormalized densities of the training data because long-run MCMC samples differ greatly from observed images. We show that it is much harder to train a ConvNet potential to learn a steady-state over realistic images. To our knowledge, long-run MCMC samples of all previous models lose the realism of short-run samples. With correct tuning of Langevin noise, we train the first ConvNet potentials for which long-run and steady-state MCMC samples are realistic images.

## 1 Introduction

### 1.1 Diagnosing Energy-Based Models

Statistical modeling of high-dimensional signals is a challenging task encountered in many academic disciplines and practical applications. We study image signals in this work. When images come without annotations or labels, the effective tools of deep supervised learning cannot be applied and

Copyright © 2020, Association for the Advancement of Artificial Intelligence (www.aaai.org). All rights reserved.

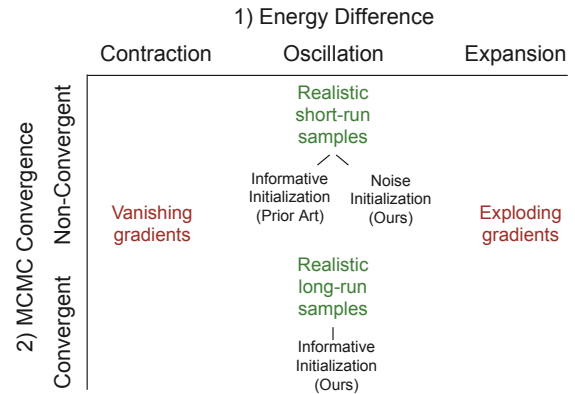


Figure 1: Two axes characterize ML learning of ConvNet potential energy functions: 1) energy difference between data samples and synthesized samples, and 2) MCMC convergence towards steady-state. Learning a sampler with realistic short-run MCMC synthesis is surprisingly simple whereas learning an energy with realistic long-run samples requires proper MCMC implementation. We propose: a) short-run training with noise initialization of the Markov chains, and b) an explanation and implementation of correct tuning for training models with realistic long-run samples.

unsupervised techniques must be used instead. This work focuses on the unsupervised paradigm of the energy-based model (1) with a ConvNet potential function (2).

Previous works studying Maximum Likelihood (ML) training of ConvNet potentials, such as (Xie et al. 2016; 2018a; Gao et al. 2018), use Langevin MCMC samples to approximate the gradient of the unknown and intractable log partition function during learning. The authors universally find that after enough model updates, MCMC samples generated by short-run Langevin from *informative initialization* (see Section 2.3) are realistic images that resemble the data.

However, we find that energy functions learned by prior works have a major defect regardless of MCMC initialization, network structure, and auxiliary training parameters.

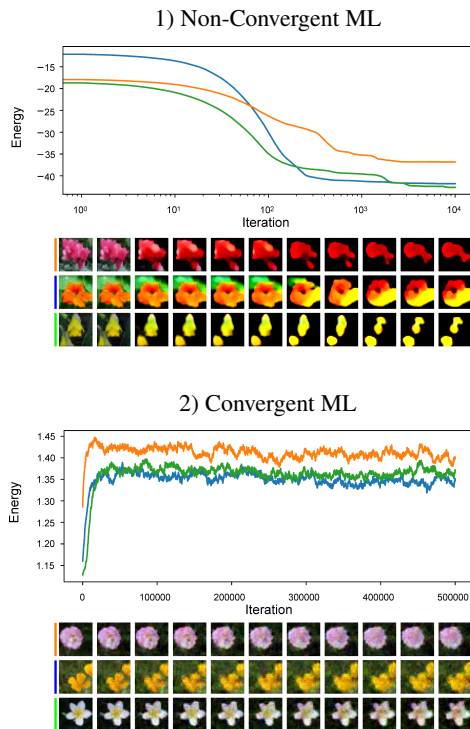


Figure 2: Long-run MH-adjusted Langevin paths from data samples to metastable samples for the Oxford Flowers 102 dataset. Models were trained with two variations of Algorithm 1: non-convergent ML trained with  $L = 100$  MCMC steps from noise initialization (*top*), and convergent ML trained with  $L = 500$  MCMC steps from persistent initialization (*bottom*).

The long-run and steady-state MCMC samples of energy functions from all previous implementations are oversaturated images with significantly lower energy than the observed data (see Figure 2 top, and Figure 3). In this case it is not appropriate to describe the learned model as an approximate density for the training set because the model assigns disproportionately high probability mass to images which differ dramatically from observed data. The systematic difference between high-quality short-run samples and low-quality long-run samples is a crucial phenomenon that appears to have gone unnoticed in previous studies.

## 1.2 Our Contributions

In this work, we present a fundamental understanding of learning ConvNet potentials by MCMC-based ML. We diagnose previously unrecognized complications that arise during learning and distill our insights to train models with new capabilities. Our main contributions are:

- Identification of two distinct axes which characterize each parameter update in MCMC-based ML learning: 1) energy difference of positive and negative samples, and 2) MCMC convergence or non-convergence. Contrary to common expectations, convergence is *not* needed for



Figure 3: Long-run Langevin samples of recent energy-based models. Probability mass is concentrated on images that have unrealistic appearance. From left to right: Wasserstein-GAN critic on Oxford flowers (Arjovsky, Chintala, and Bottou 2017), WINN on Oxford flowers (Lee et al. 2018), conditional EBM on ImageNet (Du and Mordatch 2019). The W-GAN critic is not trained to be an unnormalized density but we include samples for reference.

high-quality synthesis. See Figure 1 and Section 3.

- The first ConvNet potentials trained using ML with purely noise-initialized MCMC. Unlike prior models, our model can efficiently generate realistic and diverse samples after training from noise alone. See Figure 7. This method is further explored in our companion work (Nijkamp et al. 2019).
- The first ConvNet potentials with realistic steady-state samples. To our knowledge, ConvNet potentials with realistic MCMC sampling in the image space are unobtainable by all previous training implementations. We refer to (Kumar et al. 2019) for a discussion. See Figure 2 (bottom) and Figure 8 (middle and right column).
- Mapping the macroscopic structure of image space energy functions using diffusion in a magnetized energy landscape for unsupervised cluster discovery. See Figure 9.

## 1.3 Related Work

**Energy-Based Image Models** Energy-based models define an unnormalized probability density over a state space to represent the distribution of states in a given system. The Hopfield network (Hopfield 1982) adapted the Ising energy model into a model capable of representing arbitrary observed data. The RBM (Restricted Boltzmann Machine) (Hinton 2012) and FRAME (Filters, Random field, And Maximum Entropy) (Zhu, Wu, and Mumford 1998; Wu, Zhu, and Liu 2000) models introduce energy functions with greater representational capacity. The RBM uses hidden units which have a joint density with the observable image pixels. The FRAME model uses convolutional filters and histogram matching to learn data features.

The pioneering work (Hinton et al. 2006) studies the hierarchical energy-based model. (Ngiam et al. 2011) is an important early work proposing feedforward neural networks to model energy functions. The energy-based model in the form of (2) is introduced in (Dai, Lu, and Wu 2015). Deep variants of the FRAME model (Xie et al. 2016; Lu, Zhu, and Wu 2016) are the first to achieve realistic synthesis with a ConvNet potential and Langevin sampling. Similar methods are applied in (Du and Mordatch 2019).

The Multi-grid model (Gao et al. 2018) learns an ensemble of ConvNet potentials for images of different scales. Learning a ConvNet potential with a generator network as approximate direct sampler is explored in (Kim and Bengio 2016; Dai et al. 2017; Xie et al. 2018b; 2018a; Han et al. 2019; Kumar et al. 2019). The works (Jin, Lazarow, and Tu 2017; Lazarow, Jin, and Tu 2017; Lee et al. 2018) learn a ConvNet potential in a discriminative framework.

Although many of these works claim to train the energy (2) to be an approximate unnormalized density for the observed images, the resulting energy functions do not have a steady-state that reflects the data (see Figure 3). Short-run Langevin samples from informative initialization are presented as approximate steady-state samples, but further investigation shows long-run Langevin consistently disrupts the realism of short-run images. Our work is the first to address and remedy the systematic non-convergence of all prior implementations.

**Energy Landscape Mapping** The full potential of the energy-based model lies in the structure of the energy landscape. Hopfield observed that the energy landscape is a model of associative memory (Hopfield 1982). Diffusion along the potential energy manifold is analogous to memory recall because the diffusion process will gradually refine a high-energy image (an incomplete or corrupted memory) until it reaches a low-energy metastable state, which corresponds to the revised memory. Techniques for mapping and visualizing the energy landscape of non-convex functions in the physical chemistry literature (Becker and Karplus 1997; Das and Wales 2017) have been applied to map the latent space of Cooperative Networks (Hill, Nijkamp, and Zhu 2019). Defects in the energy function (2) from previous ML implementations prevent these techniques from being applied in the image space. Our convergent ML models enable image space mapping.

## 2 Learning Energy-Based Models

In this section, we review the established principles of the MCMC-based ML learning from prior works such as (Hinton 2002; Zhu, Wu, and Mumford 1998; Xie et al. 2016).

### 2.1 Maximum Likelihood Estimation

An energy-based model is a Gibbs-Boltzmann density

$$p_\theta(x) = \frac{1}{Z(\theta)} \exp\{-U(x; \theta)\} \quad (1)$$

over signals  $x \in \mathcal{X} \subset \mathbb{R}^N$ . The energy potential  $U(x; \theta)$  belongs to a parametric family  $\mathcal{U} = \{U(\cdot; \theta) : \theta \in \Theta\}$ . The intractable constant  $Z(\theta) = \int_{\mathcal{X}} \exp\{-U(x; \theta)\} dx$  is never used explicitly because the potential  $U(x; \theta)$  provides sufficient information for MCMC sampling. In this paper we focus our attention on energy potentials with the form

$$U(x; \theta) = F(x; \theta) \quad (2)$$

where  $F(x; \theta)$  is a convolutional neural network with a single output channel and weights  $\theta \in \mathbb{R}^D$ .

In ML learning, we seek to find  $\theta \in \Theta$  such that the parametric model  $p_\theta(x)$  is a close approximation of the data distribution  $q(x)$ . One measure of closeness is the Kullback-Leibler (KL) divergence. Learning proceeds by solving

$$\begin{aligned} \arg \min_{\theta} \mathcal{L}(\theta) &= \arg \min_{\theta} D_{KL}(q \| p_\theta) \\ &= \arg \min_{\theta} \{\log Z(\theta) + E_q[U(X; \theta)]\}. \end{aligned} \quad (3)$$

We can minimize  $\mathcal{L}(\theta)$  by finding the roots of the derivative

$$\frac{d}{d\theta} \mathcal{L}(\theta) = \frac{d}{d\theta} \log Z(\theta) + \frac{d}{d\theta} E_q[U(X; \theta)]. \quad (5)$$

The term  $\frac{d}{d\theta} \log Z(\theta)$  is intractable, but it can be expressed

$$\frac{d}{d\theta} \log Z(\theta) = -E_{p_\theta} \left[ \frac{\partial}{\partial \theta} U(X; \theta) \right]. \quad (6)$$

The gradient used to learn  $\theta$  then becomes

$$\begin{aligned} \frac{d}{d\theta} \mathcal{L}(\theta) &= \frac{d}{d\theta} E_q[U(X; \theta)] - E_{p_\theta} \left[ \frac{\partial}{\partial \theta} U(X; \theta) \right] \\ &\approx \frac{\partial}{\partial \theta} \left( \frac{1}{n} \sum_{i=1}^n U(X_i^+; \theta) - \frac{1}{m} \sum_{i=1}^m U(X_i^-; \theta) \right) \end{aligned} \quad (7)$$

(8)

where  $\{X_i^+\}_{i=1}^n$  are i.i.d. samples from the data distribution  $q$  (called *positive* samples since probability is increased), and  $\{X_i^-\}_{i=1}^m$  are i.i.d. samples from current learned distribution  $p_\theta$  (called *negative* samples since probability is decreased). In practice, the positive samples  $\{X_i^+\}_{i=1}^n$  are a batch of training images and the negative samples  $\{X_i^-\}_{i=1}^m$  are obtained after  $L$  iterations of MCMC sampling.

### 2.2 MCMC Sampling with Langevin Dynamics

Obtaining the negative samples  $\{X_i^-\}_{i=1}^m$  from the current distribution  $p_\theta$  is a computationally intensive task which must be performed for each update of  $\theta$ . ML learning does not impose a specific MCMC algorithm. Early energy-based models such as the RBM and FRAME model use Gibbs sampling as the MCMC method. Gibbs sampling updates each dimension (one pixel of the image) sequentially. This is computationally infeasible when training an energy with the form (2) for standard image sizes.

Several works studying the energy (2) recruit Langevin Dynamics to obtain the negative samples (Xie et al. 2016; Lu, Zhu, and Wu 2016; Xie et al. 2018a; Gao et al. 2018; Lee et al. 2018). The Langevin Equation

$$X_{\ell+1} = X_\ell - \frac{\varepsilon^2}{2} \frac{\partial}{\partial x} U(X_\ell; \theta) + \varepsilon Z_\ell, \quad (9)$$

where  $Z_\ell \sim N(0, I_N)$  and  $\varepsilon > 0$ , has stationary distribution  $p_\theta$  (Geman and Geman 1984; Neal 2011). A complete implementation of Langevin Dynamics requires a momentum update and Metropolis-Hastings update in addition to (9), but most authors find that these can be ignored in practice for small enough  $\varepsilon$  (Chen, Fox, and Guestrin 2014).

Like most MCMC methods, Langevin dynamics exhibits high auto-correlation and has difficulty mixing between separate modes. Even so, long-run Langevin samples with a suitable initialization can still be considered approximate steady-state samples, as discussed next.

### 2.3 MCMC Initialization

We distinguish two main branches of MCMC initialization: *informative initialization*, where the density of initial states is meant to approximate the model density, and *non-informative initialization*, where initial states are obtained from a distribution that is unrelated to the model density. *Noise initialization* is a specific type of non-informative initialization where initial states come from a noise distribution such as uniform or Gaussian.

In the most extreme case, a Markov chain initialized from its steady-state will follow the steady-state distribution after a single MCMC update. In more general cases, a Markov chain initialized from an image that is likely under the steady-state can converge much more quickly than a Markov chain initialized from noise. For this reason, all prior works studying ConvNet potentials use informative initialization.

*Data-based initialization* uses samples from the training data as the initial MCMC states. Contrastive Divergence (CD) (Hinton 2002) introduces this practice. The Multigrid Model (Gao et al. 2018) generalizes CD by using multi-scale energy functions to sequentially refine downsampled data.

*Persistent initialization* uses negative samples from a previous learning iteration as initial MCMC states in the current iteration. The persistent chains can be initialized from noise as in (Zhu, Wu, and Mumford 1998; Lu, Zhu, and Wu 2016; Xie et al. 2016) or from data samples as in Persistent Contrastive Divergence (PCD) (Tieleman 2008). The Cooperative Learning model (Xie et al. 2018a) generalizes persistent chains by learning a generator for proposals in tandem with the energy.

In this paper we consider long-run Langevin chains from both data-based initialization such as CD and persistent initialization such as PCD to be approximate steady-state samples, even when Langevin chains cannot mix between modes. Prior art indicates that both initialization types span the modes of the learned density, and long-run Langevin samples will travel in a way that respects the  $p_\theta$  in the local landscape.

Informative MCMC initialization during ML training can limit the ability of the final model  $p_\theta$  to generate new and diverse synthesized images after training. MCMC samples initialized from noise distributions after training tend to result in images with a similar type of appearance when informative initialization is used in training.

In contrast to common wisdom, we find that informative initialization is not necessary for efficient and realistic synthesis when training ConvNet potentials with ML. In accordance with common wisdom, we find that informative initialization is essential for learning a realistic steady-state.

## 3 Two Axes of ML Learning

Inspection of the gradient (8) reveals the central role of the difference of the average energy of negative and positive samples. Let

$$d_{s_t}(\theta) = E_q[U(X; \theta)] - E_{s_t}[U(X; \theta)] \quad (10)$$

where  $s_t(x)$  is the distribution of negative samples given the finite-step MCMC sampler and initialization used at training

step  $t$ . The difference  $d_{s_t}(\theta)$  measures whether the positive samples from the data distribution  $q$  or the negative samples from  $s_t$  are more likely under the model  $p_\theta$ . The ideal case  $p_\theta = q$  (perfect learning) and  $s_t = p_\theta$  (exact MCMC convergence) satisfies  $d_{s_t}(\theta) = 0$ . A large value of  $|d_{s_t}|$  indicates that either learning or sampling (or both) have not converged.

Although  $d_{s_t}(\theta)$  is not equivalent to the ML objective (4), it bridges the gap between theoretical ML and the behavior encountered when MCMC approximation is used. Two outcomes occur for each update on the parameter path  $\{\theta_t\}_{t=1}^{T+1}$ :

1.  $d_{s_t}(\theta_t) < 0$  (expansion) or  $d_{s_t}(\theta_t) > 0$  (contraction)
2.  $s_t \approx p_{\theta_t}$  (MCMC convergence) or  $s_t \not\approx p_{\theta_t}$  (MCMC non-convergence).

We find that only the first axis governs the stability and synthesis results of the learning process. Oscillation of expansion and contraction updates is an indicator of stable ML learning, but this can occur in cases where either  $s_t$  is always approximately convergent or where  $s_t$  never converges.

Behavior along the second axis determines the realism of steady-state samples from the final learned energy. Samples from  $p_{\theta_t}$  will be realistic if and only if  $s_t$  has realistic samples and  $s_t \approx p_{\theta_t}$ . We use *convergent ML* to refer to implementations where  $s_t \approx p_{\theta_t}$  for all  $t > t_0$ , where  $t_0$  represents burn-in learning steps (e.g. early stages of persistent learning). We use *non-convergent ML* to refer to all other implementations. All prior ConvNet potentials are learned with non-convergent ML, although this is not recognized by previous authors.

Without proper tuning of the sampling phase, the learning heavily gravitates towards non-convergent ML. In this section we outline principles to explain this behavior and provide a remedy for the tendency of model non-convergence.

### 3.1 First Axis: Expansion or Contraction

Following prior art for high-dimensional image models, we use the Langevin Equation (9) to obtain MCMC samples. Let  $w_t$  give the joint distribution of a Langevin chain  $(Y_t^{(0)}, \dots, Y_t^{(L)})$  at training step  $t$ , where  $Y_t^{(\ell+1)}$  is obtained by applying (9) to  $Y_t^{(\ell)}$  and  $Y_t^{(L)} \sim s_t$ . Since the gradient  $\frac{\partial U}{\partial x}$  appears directly in the Langevin equation, the quantity

$$v_t = E_{w_t} \left[ \frac{1}{L+1} \sum_{\ell=0}^L \left\| \frac{\partial}{\partial y} U(Y_t^{(\ell)}; \theta_t) \right\|_2 \right],$$

which gives the average image gradient magnitude of  $U$  along an MCMC path at training step  $t$ , plays a central role in sampling. Sampling at noise magnitude  $\varepsilon$  will lead to very different behavior depending on the gradient magnitude. If  $v_t$  is very large, gradients will overwhelm the noise and the resulting dynamics are similar to gradient descent. If  $v_t$  is very small, sampling becomes an isotropic random walk. A valid image density should appropriately balance energy gradient magnitude and noise strength to enable realistic long-run sampling.

We empirically observe that expansion and contraction updates tend to have opposite effects on  $v_t$  (see Figure 4).

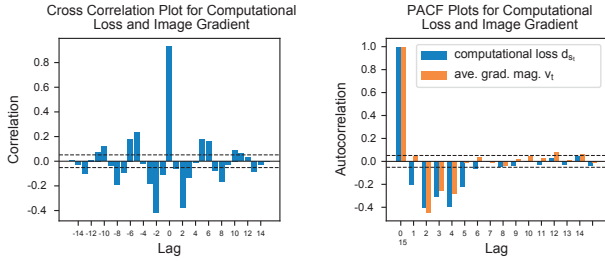


Figure 4: Illustration of expansion/contraction oscillation for a single training implementation. This behavior is typical of convergent *and* non-convergent ML. *Left*: Cross correlation of  $d_{s_t}$  (uncentered) and  $v_t$  (mean centered). The two are highly correlated at lag 0 and exhibit negative correlation for lag  $\pm 3$  steps, indicating that expansion updates tend to increase gradient strength in the near future and vice-versa. *Right*: PACF plots of  $d_{s_t}$  (uncentered) and  $v_t$  (mean centered). Both have a strong negative autocorrelation within the next 4 training batches, showing that expansion updates tend to follow contraction updates and vice-versa.

Gradient magnitude  $v_t$  and computational loss  $d_{s_t}$  are highly correlated at the current iteration and exhibit significant negative correlation at a short-range lag. Both have significant negative autocorrelation for short-range lag. This indicates that expansion updates tend to increase  $v_t$  and contraction updates tend to decrease  $v_t$ , and that expansion updates tend to lead to contraction updates and vice-versa. We believe that the natural oscillation between expansion and contraction updates underlies the stability of ML with (2).

Learning can become unstable when  $U$  is updated in the expansion phase for many consecutive iterations if  $v_t \rightarrow \infty$  and as  $U(X^+) \rightarrow -\infty$  for positive samples and  $U(X^-) \rightarrow \infty$  for negative samples. This behavior is typical of W-GAN training (interpreting the generator as  $w_t$  with  $L = 0$ ) and the W-GAN Lipschitz bound is needed to prevent such instability. In ML learning with ConvNet potentials, consecutive updates in the expansion phase will increase  $v_t$  so that the gradient can better overcome noise and samples can more quickly reach low-energy regions. In contrast, many consecutive contraction updates can cause  $v_t$  to shrink to 0, leading to the solution  $U(x) = c$  for some constant  $c$  (see Figure 5 right, blue lines). In proper ML learning, the expansion updates that follow contraction updates prevent the model from collapsing to a flat solution and force  $U$  to learn meaningful features of the data.

Throughout our experiments, we find that the network can easily learn to balance the energy of the positive and negative samples so that  $d_{s_t}(\theta_t) \approx 0$  after only a few model updates. In fact, ML learning can easily adjust  $v_t$  so that the gradient is strong enough to balance  $d_{s_t}$  and obtain high-quality samples from virtually *any* initial distribution in a small number of MCMC steps. This insight leads to our ML method with noise-initialized MCMC. The natural oscillation of ML learning is the foundation of the robust synthesis capabilities of ConvNet potentials, but realistic short-run MCMC samples can mask the true steady-state behavior.

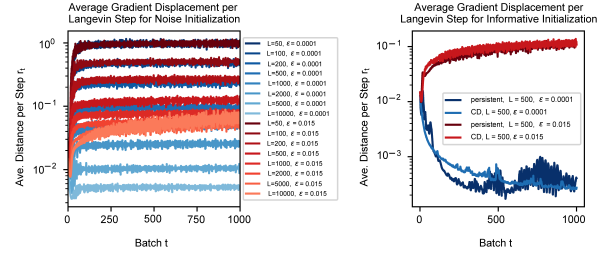


Figure 5: Illustration of gradient strength for convergent and non-convergent ML. With low noise (blue) the energy either learns only the burn-in path (left) or contracts to a constant function (right). With sufficient noise (red), the network gradient learns to balance with noise magnitude and it becomes possible to learn a realistic steady-state.

### 3.2 Second Axis: MCMC Convergence or Non-Convergence

In the literature, it is expected that the finite-step MCMC distribution  $s_t$  must approximately converge to its steady-state  $p_{\theta_t}$  for learning to be effective. On the contrary, we find that high-quality synthesis is possible, and actually easier to learn, when there is a drastic difference between the finite-step MCMC distribution  $s_t$  and true steady-state samples of  $p_{\theta_t}$ . An examination of ConvNet potentials learned by existing methods shows that in all cases, running the MCMC sampler for significantly longer than the number of training steps results in samples with significantly lower energy and unrealistic appearance. Although synthesis is possible without convergence, it is not appropriate to describe a non-convergent ML model  $p_{\theta}$  as an approximate data density.

Oscillation of expansion and contraction updates occurs for both convergent and non-convergent ML learning, but for very different reasons. In convergent ML, we expect the average gradient magnitude  $v_t$  to converge to a constant that is balanced with the noise magnitude  $\epsilon$  at a value that reflects the temperature of the data density  $q$ . However, ConvNet potentials can circumvent this desired behavior by tuning  $v_t$  with respect to the burn-in energy landscape rather than noise  $\epsilon$ . Figure 5 shows how average image space displacement  $r_t = \frac{\epsilon^2}{2} v_t$  is affected by noise magnitude  $\epsilon$  and number of Langevin steps  $L$  for noise, data-based, and persistent MCMC initializations.

For noise initialization with low  $\epsilon$ , the model adjusts  $v_t$  so that  $r_t L \approx R$  where  $R$  is the average distance between an image from the noise initialization distribution and an image from the data distribution. In other words, the MCMC paths obtained from non-convergent ML with noise initialization are nearly linear from the starting point to the ending point. Mixing does *not* improve when  $L$  increases because  $r_t$  shrinks in proportion to the increase. Oscillation of expansion and contraction updates occurs because the model tunes  $v_t$  to control how far along the burn-in path the negative samples travel. Samples never reach the steady-state energy spectrum and MCMC mixing is not possible.

For data initialization and persistent initialization with

low  $\varepsilon$ , we see that  $v_t, r_t \rightarrow 0$  and that learning tends to the trivial solution  $U(x) = c$ . This occurs because contraction updates dominate the learning dynamics. At low  $\varepsilon$ , samples initialized from the data will easily have lower energy than the data since sampling reduces to gradient descent. To our knowledge no authors have trained (2) using CD, possibly because the energy can easily collapse to a trivial flat solution. For persistent learning, the model learns to synthesize meaningful features early in learning and then contracts in gradient strength once it becomes easy to find negative samples with lower energy than the data. Previous authors who trained models with persistent chains use auxiliary techniques such as a Gaussian prior (Xie et al. 2016) or occasional rejuvenation of chains from noise (Du and Mor-datch 2019) which prevent unbalanced network contraction, although the role of these techniques is not recognized by the authors.

For all three initialization types, we can see that convergent ML becomes possible when  $\varepsilon$  is large enough. ML with noise initialization behaves similarly for high and low  $\varepsilon$  when  $L$  is small. For large  $L$  with high  $\varepsilon$ , the model tunes  $v_t$  to balance with  $\varepsilon$  rather than  $R/L$ . The MCMC samples complete burn-in and begin to mix for large  $L$ , and increasing  $L$  will indeed lead to improved MCMC convergence as usual. For data-based and persistent initialization, we see that  $v_t$  adjusts to balance with  $\varepsilon$  instead of contracting to 0 because the noise added during Langevin sampling forces  $U$  to learn meaningful features.

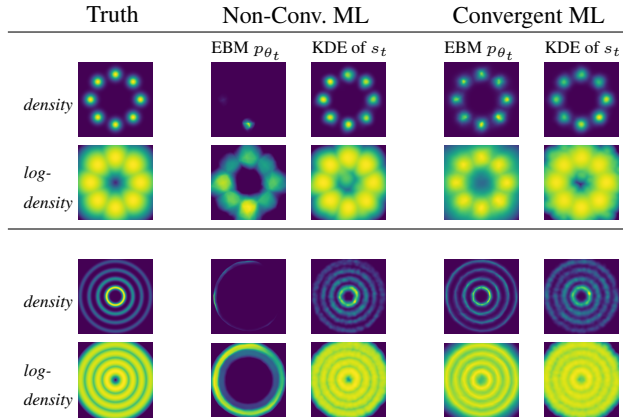


Figure 6: Comparison of convergent and non-convergent ML for 2D toy distributions. Non-convergent ML does not learn a valid density but the kernel density estimate of the negative samples reflects the groundtruth. Convergent ML learns an energy that closely approximates the true density.

### 3.3 Learning Algorithm

We now present an algorithm for ML learning. The algorithm is essentially the same as earlier works such as (Xie et al. 2016) that investigate the potential (2). Our intention is not to introduce a novel algorithm but to demonstrate the range of phenomena that can occur with the ML objective

based on changes to MCMC sampling. We present guidelines for the effect of tuning on the learning outcome.

---

#### Algorithm 1: ML Learning

---

**input** : ConvNet potential  $U(x; \theta)$ , number of training steps  $T$ , initial weight  $\theta_1$ , training images  $\{x_i^+\}_{i=1}^{N_{\text{data}}}$ , step size  $\varepsilon$ , noise indicator  $\tau \in \{0, 1\}$ , Langevin steps  $L$ , learning rate  $\gamma$ .  
**output**: Weights  $\theta_{T+1}$  for energy  $U(x; \theta)$ .  
**for**  $t = 1 : T$  **do**

1. Draw batch images  $\{X_i^+\}_{i=1}^n$  from training set.  
 Draw initial negative samples  $\{Y_i^{(0)}\}_{i=1}^m$  from MCMC initialization method (noise or informative initialization, see Section 2.3).

2. Update  $\{Y_i^{(0)}\}_{i=1}^m$  with

$$Y_i^{(\ell)} = Y_i^{(\ell-1)} - \frac{\varepsilon^2}{2} \frac{\partial}{\partial y} U(Y_i^{(\ell-1)}; \theta_t) + \varepsilon \tau Z_{i,\ell},$$

where  $Z_{i,\ell} \sim \mathcal{N}(0, I_N)$ , for  $L$  steps to obtain

negative samples  $\{X_i^-\}_{i=1}^m = \{Y_i^{(L)}\}_{i=1}^m$ .  
 3. Update the weights by  $\theta_{t+1} = \theta_t - g(\Delta\theta_t, \gamma)$  where  $\Delta\theta_t$  is the stochastic gradient (8) and  $g$  is the SGD or Adam (Kingma and Ba 2015) optimizer.

---

- *Noise and Step Size for Non-Convergent ML*: For non-convergent training we find the tuning of noise and step-size have little effect on training stability. We use  $\varepsilon = 1$  and  $\tau = 0$ . Noise is not needed for oscillation because  $d_{s_t}$  is controlled by the depth of samples along the burn-in path. Including low noise appears to improve synthesis quality.
- *Noise and Step Size for Convergent ML*: For convergent training, we find that it is essential to include noise with  $\tau = 1$  and precisely tune  $\varepsilon$  so that the network learns true mixing dynamics through the gradient strength. The step size  $\varepsilon$  should approximately match the local standard deviation of the data along the most constrained direction (Neal 2011). An effective  $\varepsilon$  for  $32 \times 32$  images with pixel values in  $[-1, 1]$  appears to lie around 0.015.
- *Number of Steps*: When  $\tau = 0$  or  $\tau = 1$  and  $\varepsilon$  is very small, learning leads to similar non-convergent ML outcomes for any  $L \geq 100$ . When  $\tau = 1$  and  $\varepsilon$  is correctly tuned, sufficiently high values of  $L$  lead to convergent ML and lower values of  $L$  lead to non-convergent ML.
- *Informative Initialization*: Informative MCMC initialization is not needed for non-convergent ML even with as few as  $L = 100$  Langevin updates. The model can naturally learn fast pathways to realistic negative samples from an arbitrary initial distribution. On the other hand, informative initialization can greatly reduce the magnitude of  $L$  needed for convergent ML. We use persistent initialization starting from noise.



Figure 7: Short-run samples obtained from an energy function trained with non-convergent ML with noise initialization. The images are generated using 100 Langevin updates from uniform noise initialization. Contrary to prior art, informative initialization is not needed for high-quality synthesis. From left to right: MNIST, Oxford Flowers 102, CelebA, CIFAR-10.

- *Network structure*: For the first convolutional layer, we observe that a  $3 \times 3$  convolution with stride 1 helps to avoid checkerboard patterns or other artifacts. For convergent ML, use of non-local layers (Wang et al. 2018) appears to improve synthesis realism.
- *Regularization and Normalization*: Previous studies employ a variety of auxiliary training techniques such as prior distributions (e.g. Gaussian), weight regularization, batch normalization, layer normalization, and spectral normalization to stabilize sampling and weight updates. We find that these techniques are not needed.
- *Optimizer and Learning Rate*: For non-convergent ML, Adam improves training speed and image quality. Our non-convergent models use Adam with  $\gamma = 0.0001$ . For convergent ML, Adam appears to interfere with learning a realistic steady-state and we use SGD instead. When using SGD with  $\tau = 1$  and properly tuned  $\varepsilon$  and  $L$ , higher values of  $\gamma$  lead to non-convergent ML and sufficiently low values of  $\gamma$  lead to convergent ML.

## 4 Experiments

### 4.1 Low-Dimensional Toy Experiments

We first demonstrate the outcomes of convergent and non-convergent ML for low-dimensional toy distributions (Figure 6). Both toy models have a standard deviation of 0.15 along the most constrained direction, and the ideal step size for Langevin dynamics is close to this value (Neal 2011). Non-convergent models are trained using noise MCMC initialization with  $L = 100$  and  $\varepsilon = 0.01$  (too low for the data temperature) and convergent models are trained using persistent MCMC initialization with  $L = 500$  and  $\varepsilon = 0.125$  (approximately the right magnitude relative to the data temperature). The distributions of the short-run samples from the non-convergent models reflect the ground-truth densities, but the learned densities are sharply concentrated and different from the ground-truths. In higher dimensions this sharp concentration of non-convergent densities manifests as oversaturated long-run images. With sufficient Langevin noise, one can learn an energy function that closely approximates the ground-truth.

### 4.2 Synthesis from Noise with Non-Convergent ML Learning

In this experiment, we learn an energy function (2) using ML with uniform noise initialization and short-run MCMC. We apply our ML algorithm with  $L = 100$  Langevin steps starting from uniform noise images for each update of  $\theta$  with  $\tau = 0$  and  $\varepsilon = 1$ . We use Adam with  $\gamma = 0.0001$ .

Previous authors argued that informative MCMC initialization is a key element for successful synthesis with ML learning, but our learning method can sample from scratch with the same Langevin budget. Unlike the models learned by previous authors, our models can generate high-fidelity and diverse images from a noise signal. Our results are shown in Figure 7, Figure 8 (left), and Figure 2 (top). Our recent companion work (Nijkamp et al. 2019) thoroughly explores the capabilities of noise-initialized non-convergent ML.

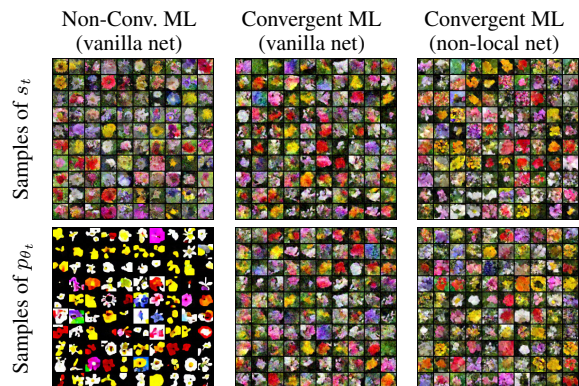


Figure 8: Comparison of negative samples and steady-state samples. Method: non-convergent ML using noise initialization and 100 Langevin steps (*left*), convergent ML with a vanilla ConvNet, persistent initialization and 500 Langevin steps (*center*), and convergent ML with a non-local net, persistent initialization and 500 Langevin steps (*right*).

### 4.3 Convergent ML Learning

With the correct Langevin noise, one can ensure that MCMC samples mix in the steady-state energy spectrum throughout training. The model will eventually learn a realistic steady-state as long as MCMC samples approximately converge for each parameter update  $t$  beyond a burn-in period  $t_0$ . One can implement convergent ML with noise initialization, but we find that this requires  $L \approx 20,000$  steps.

Informative initialization can dramatically reduce the number of MCMC steps needed for convergent learning. By using SGD with learning rate  $\gamma = 0.0005$ , noise indicator  $\tau = 1$  and step size  $\varepsilon = 0.015$ , we were able to train convergent models using persistent initialization and  $L = 500$  sampling steps. We initialize 10,000 persistent images from noise and update 100 images for each batch. We implement the same training procedure for a vanilla ConvNet and a network with non-local layers (Wang et al. 2018). Our results are shown in Figure 8 (middle, right) and Figure 2 (bottom).

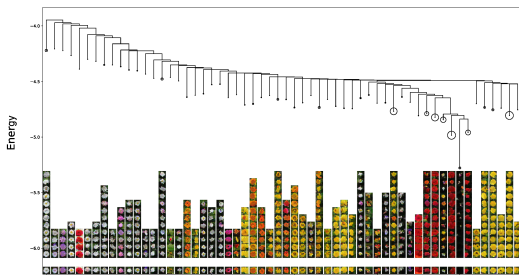


Figure 9: Visualization of basin structure of the learned energy function  $U(x)$  for the Oxford Flowers 102 dataset. Columns display randomly selected basin members and circles indicate the total number of basin members. Vertical lines encode basin minimum energy and horizontal lines depict the lowest known barrier at which two basins merge.

### 4.4 Mapping the Image Space

A well-formed energy function partitions the image space into meaningful Hopfield basins of attraction. Following Algorithm 3 of (Hill, Nijkamp, and Zhu 2019), we map the structure of a convergent energy. We first identify many metastable MCMC samples. We then sort the metastable samples from lowest energy to highest energy and sequentially group images if travel between samples is possible in a magnetized energy landscape. This process is continued until all minima have been clustered. Our mappings show that the convergent energy has meaningful metastable structures encoding recognizable concepts (Figure 9).

## 5 Conclusion and Future Work

Our experiments on energy-based models with the form (2) reveal two distinct axes of ML learning. We use our insights to train models with sampling capabilities that are unobtainable by previous implementations. The informative MCMC initializations used by previous authors are not necessary for high-quality synthesis. By removing this tech-

nique we train the first energy functions capable of high-diversity and realistic synthesis from noise initialization after training. We identify a severe defect in the steady-state distributions of prior implementations and introduce the first ConvNet potentials of the form (2) for which steady-state samples have realistic appearance. Our observations could be very useful for convergent ML learning with more complex MCMC initialization methods used in (Xie et al. 2018a; Gao et al. 2018). We hope that our work paves the way for future unsupervised and weakly supervised applications with energy-based models.

### Acknowledgment

The work is supported by DARPA XAI project N66001-17-2-4029; ARO project W911NF1810296; and ONR MURI project N00014-16-1-2007; and Extreme Science and Engineering Discovery Environment (XSEDE) grant ASC170063. We thank Prafulla Dhariwal and Anirudh Goyal for helpful discussions.

### References

- Arjovsky, M.; Chintala, S.; and Bottou, L. 2017. Wasserstein generative adversarial networks. In *Proceedings of the 34th International Conference on Machine Learning, ICML*, 214–223.
- Becker, O. M., and Karplus, M. 1997. The topology of multidimensional potential energy surfaces: Theory and application to peptide structure and kinetics. *Journal of Chemical Physics* 106(4):1495–1517.
- Chen, T.; Fox, E. B.; and Guestrin, C. 2014. Stochastic gradient hamiltonian monte carlo. In *Proceedings of the 31th International Conference on Machine Learning, ICML*, 1683–1691.
- Dai, Z.; Almahairi, A.; Bachman, P.; Hovy, E. H.; and Courville, A. C. 2017. Calibrating energy-based generative adversarial networks. In *5th International Conference on Learning Representations, ICLR*.
- Dai, J.; Lu, Y.; and Wu, Y. N. 2015. Generative modeling of convolutional neural networks. In *3rd International Conference on Learning Representations, ICLR*.
- Das, R., and Wales, D. J. 2017. Machine learning landscapes for patient outcome. *Royal Society Open Science* 4:16600–16605.
- Du, Y., and Mordatch, I. 2019. Implicit generation and generalization in energy-based models. *Advances in Neural Information Processing Systems 33, NeurIPS*.
- Gao, R.; Lu, Y.; Zhou, J.; Zhu, S.; and Wu, Y. N. 2018. Learning generative convnets via multi-grid modeling and sampling. In *IEEE Conference on Computer Vision and Pattern Recognition, CVPR*, 9155–9164.
- Geman, S., and Geman, D. 1984. Stochastic relaxation, gibbs distributions, and the bayesian restoration of images. *IEEE Trans. Pattern Anal. Mach. Intell.* 6(6):721–741.
- Han, T.; Nijkamp, E.; Fang, X.; Hill, M.; Zhu, S.-C.; and Wu, Y. N. 2019. Divergence triangle for joint training of generator model, energy-based model, and inferential



- model. In *The IEEE Conference on Computer Vision and Pattern Recognition, CVPR*.
- Hill, M.; Nijkamp, E.; and Zhu, S.-C. 2019. Building a telescope to look into high-dimensional image spaces. *QAM* 77(2):269–321.
- Hinton, G. E.; Osindero, S.; Welling, M.; and Teh, Y. W. 2006. Unsupervised discovery of nonlinear structure using contrastive backpropagation. *Cognitive Science* 30(4):725–731.
- Hinton, G. E. 2002. Training products of experts by minimizing contrastive divergence. *Neural Computation* 14(8):1771–1800.
- Hinton, G. E. 2012. A practical guide to training restricted boltzmann machines. In *Neural Networks: Tricks of the Trade - Second Edition*. 599–619.
- Hopfield, J. J. 1982. Neural networks and physical systems with emergent collective computational abilities. In *Proceedings of the national academy of sciences*, volume 79, 2554–2558. National Acad Sciences.
- Jin, L.; Lazarow, J.; and Tu, Z. 2017. Introspective learning for discriminative classification. In *Advances in Neural Information Processing Systems 31, NeurIPS*.
- Kim, T., and Bengio, Y. 2016. Deep directed generative models with energy-based probability estimation. *CoRR* abs/1606.03439.
- Kingma, D. P., and Ba, J. 2015. Adam: A method for stochastic optimization. In *3rd International Conference on Learning Representations, ICLR*.
- Kumar, R.; Goyal, A.; Courville, A. C.; and Bengio, Y. 2019. Maximum entropy generators for energy-based models. *CoRR* abs/1901.08508.
- Lazarow, J.; Jin, L.; and Tu, Z. 2017. Introspective neural networks for generative modeling. In *IEEE International Conference on Computer Vision, ICCV*, 2793–2802.
- Lee, K.; Xu, W.; Fan, F.; and Tu, Z. 2018. Wasserstein introspective neural networks. In *IEEE Conference on Computer Vision and Pattern Recognition, CVPR*, 3702–3711.
- Lu, Y.; Zhu, S.; and Wu, Y. N. 2016. Learning FRAME models using CNN filters. In *Proceedings of the Thirtieth AAAI Conference on Artificial Intelligence*, 1902–1910.
- Neal, R. M. 2011. MCMC using hamiltonian dynamics. *Handbook of Markov Chain Monte Carlo Chapter 5*.
- Ngiam, J.; Chen, Z.; Koh, P. W.; and Ng, A. Y. 2011. Learning deep energy models. In *Proceedings of the 28th International Conference on Machine Learning, ICML*, 1105–1112.
- Nijkamp, E.; Hill, M.; Zhu, S.-C.; and Wu, Y. N. 2019. Learning non-convergent non-persistent short-run MCMC toward energy-based model. *Advances in Neural Information Processing Systems 33, NeurIPS*.
- Tieleman, T. 2008. Training restricted boltzmann machines using approximations to the likelihood gradient. In *Machine Learning, Proceedings of the Twenty-Fifth International Conference ICML*, 1064–1071.
- Wang, X.; Girshick, R. B.; Gupta, A.; and He, K. 2018. Non-local neural networks. In *IEEE Conference on Computer Vision and Pattern Recognition, CVPR*, 7794–7803.
- Wu, Y. N.; Zhu, S. C.; and Liu, X. 2000. Equivalence of julesz ensembles and FRAME models. *International Journal of Computer Vision* 38(3):247–265.
- Xie, J.; Lu, Y.; Zhu, S.; and Wu, Y. N. 2016. A theory of generative convnet. In *Proceedings of the 33rd International Conference on Machine Learning, ICML*, 2635–2644.
- Xie, J.; Lu, Y.; Gao, R.; and Wu, Y. N. 2018a. Cooperative learning of energy-based model and latent variable model via MCMC teaching. In *Proceedings of the Thirty-Second AAAI Conference on Artificial Intelligence*, 4292–4301.
- Xie, J.; Lu, Y.; Gao, R.; Zhu, S.-C.; and Wu, Y. N. 2018b. Cooperative training of descriptor and generator networks. *IEEE transactions on pattern analysis and machine intelligence (PAMI)*.
- Zhu, S. C.; Wu, Y. N.; and Mumford, D. 1998. Filters, random fields and maximum entropy (FRAME): towards a unified theory for texture modeling. *International Journal of Computer Vision* 27(2):107–126.